HHS Public Access

Author manuscript

Vet Ophthalmol. Author manuscript; available in PMC 2016 May 01.

Published in final edited form as:

Vet Ophthalmol. 2015 May ; 18(3): 242–250. doi:10.1111/vop.12194.

Therapeutic potential of Pirfenidone for treating equine corneal scarring

Michael K. Fink[1,3], **Elizabeth A. Giuliano**[3], **Ashish Tandon**[1,2], and **Rajiv R. Mohan**[*,1,2,3]

[1]Harry S. Truman Memorial Veterans Hospital, Columbia, Missouri, USA

[2]Mason Eye Institute, School of Medicine, University of Missouri, Columbia, Missouri, USA

[3]College of Veterinary Medicine, University of Missouri, Columbia, Missouri, USA

Abstract

Objective—To evaluate the safety and efficacy of Pirfenidone (PFD) in the treatment of equine corneal fibrosis using an *in vitro* model.

Methods—Healthy donor equine corneas were collected and used to generate primary equine corneal fibroblasts (ECFs) by growing cultures in minimal essential medium supplemented with 10% fetal bovine serum. Equine corneal myofibroblasts (ECMs), used as a model of equine corneal fibrosis, were produced by growing ECF cultures in serum-free medium containing transforming growth factor β1 (1ng/ml). Trypan blue viability assays and changes in ECF morphology were utilized to determine the optimal PFD dose for this *in vitro* model. Trypan blue viability, phase contrast microscopy, and TUNEL assays were used to evaluate the cytotoxicity of PFD. Scratch and MTT assays were used to evaluate the effect of PFD on cellular migration and proliferation. Real-time PCR, immunoblot analysis, and immunocytochemistry were employed to determine the efficacy of PFD to inhibit ECM formation *in vitro*.

Results—Topical PFD application at 200 μg/ml successfully decreased αSMA expression when compared to the TGFβ1 only treatment group ($P < 0.01$). PFD application ≤ 200 μg/ml did not affect ECF phenotype or cellular viability and did not result in significant cytotoxicity.

Conclusions—Pirfenidone safely and effectively inhibits TGFβ1-induced equine corneal fibrosis *in vitro*. *In vivo* studies are warranted.

Keywords

equine; cornea; fibroblasts; fibrosis; myofibroblasts; pirfenidone

INTRODUCTION

Equine corneal scarring results from a variety of corneal insults, commonly affects horses worldwide, and often causes permanent vision loss. A variety of factors contribute to the frequency of this sequela including the anatomic placement and dimensions of the equine

[*]Corresponding author: Rajiv R. Mohan, PhD., FARVO Professor of Ophthalmology and Molecular Medicine University of Missouri 1600 E. Rollins St, Columbia, MO 65211 mohanr@health.missouri.edu Phone: (573) 884-1449 and Fax: (573) 884-6551.

globe, as well as the environmental conditions to which horses are commonly exposed.[1] Successful treatment of equine keratitis or corneal trauma is often costly, labor intensive, and protracted with surgical intervention and concentrated medical management regularly employed in combination.[1] Current treatment of equine corneal ulceration relies on a multifaceted therapeutic approach of topical and systemic agents administered frequently to control infection (antimicrobials and antifungals), decrease stromal degradation (anti-collagenases), inhibit ciliary spasm while stabilizing the blood-aqueous barrier (mydriatics), and alleviate ocular pain (nonsteroidal anti-inflammatory drugs).[1-3] In veterinary ophthalmology, the potential of many pharmacologic agents demonstrating significant inhibition of fibrosis in non-ocular tissues has not been evaluated in the management of equine corneal fibrosis.

Corneal wound healing is crucial for the maintenance of ocular structural integrity, corneal transparency and normal vision.[4-6] Corneal healing involves numerous cellular mechanisms including the migration, proliferation, and apoptosis of corneal epithelial cells and fibroblasts, stromal remodeling, extracellular matrix synthesis, and the transdifferentiation of fibroblasts to myofibroblasts.[7, 8] A variety of factors regulate corneal wound healing, including growth factors, cytokines, and chemokines.[9-11] Of these, transforming growth factor beta (TGFβ) acts as the primary stimulant of fibroplasia and plays a major role in converting equine corneal fibroblasts (ECFs) to equine corneal myofibroblasts (ECMs) and stimulating irregular deposition of extracellular matrix.[11] The development of corneal fibrosis and loss of corneal transparency is greatly dependent on this complex process.[12] In comparison to quiescent, crystallin-rich, transparent keratocytes, corneal myofibroblasts are opaque, highly contractile cells with decreased intracellular crystalline content.[13-15] Previous studies have demonstrated that a reduction in myofibroblast formation decreases corneal fibrosis and ultimately increases corneal transparency following corneal injury.[16-19] Due to the integral role that TGFβ plays within the wound healing process, antagonizing TGFβ in order to mediate the proliferation and transdifferentiation of fibroblasts to myofibroblasts is a promising therapeutic strategy to prevent corneal fibrosis.

Pirfenidone (5-methyl-1-phenyl-2[1H]-pyridone) has demonstrated substantial anti-fibrotic and anti-inflammatory activities both *in vitro* and *in vivo* within experimental models of disease in several major organ systems.[20-27] Mechanistically, PFD has been shown to reduce cellular proliferation, TGFβ-stimulated collagen production, and TGFβ-mediated profibrogenic factors.[21, 23] Although the exact cellular mechanism of action has yet to be determined, PFD inhibits TGFβ mRNA and protein production.[28, 29] In ocular tissues, PFD has been reported to prevent the proliferation, migration, and collagen contraction of human Tenon's fibroblasts *in vitro* while inhibiting postoperative scarring in experimental models of strabismus and glaucoma.

[23, 24] In addition, PFD has shown promise in treating hepatic cirrhosis, pulmonary fibrosis, and renal fibrosis.[20-22, 25, 26, 30] At present, the potential of PFD to treat equine corneal fibrosis has not been investigated. The purpose of this study was to examine the potential toxicity and anti-fibrotic effects of PFD in treating equine corneal fibrosis using an *in vitro* model.[31]

MATERIALS AND METHODS

Equine corneal fibroblast and myofibroblast cultures

ECFs were generated from corneal buttons that were aseptically harvested from healthy research horses undergoing humane euthanasia for reasons unrelated to this study. Prior to euthanasia, slit-lamp biomicroscopy was performed by an experienced veterinary ophthalmologist (EAG) to ensure that all samples were harvested from horses free of ocular disease. Corneas were washed with sterile minimal essential medium (MEM; Gibco, Grand Island, NY) and their epithelium and endothelium were manually removed by precise scraping using a #10 Bard Parker scalpel blade (BD, Franklin Lakes, NJ). Corneal stroma was then sectioned into five smaller explants and placed into 100×20 mm tissue culture plates (BD BioSciences, Durham, NC) containing MEM supplemented with 10% fetal bovine serum (Gibco, Grand Island, NY) and then incubated in a humidified CO_2 incubator (Thermo Scientific, Asheville, NC) at 37 °C. In approximately 3-7 days, primary fibroblasts began migrating from the stromal sub-sections. At 90% confluence, the explants were manually removed with rattoothed forceps and discarded, while confluent ECFs were trypsinized and then plated on new tissue culture plates to yield ECF cultures.

Dose-dependent studies were performed to determine the optimal dose of PFD for this investigation. PFD at concentrations of 0, 50, 100, 150, 200, and 300 μg/ml was applied to ECF cultures in serum-free MEM medium for 48 h. After 48 h, cellular viability was assessed and ECFs were observed for phenotypic changes (see cytotoxicity studies). Following preliminary dose finding studies, a PFD concentration of 200 μg/ml was used for all subsequent experiments.

To generate ECMs, ECF cultures were exposed to 1ng/ml TGFβ1 (PeproTech Inc, Rocky Hill, NJ) under serum-free conditions for 5-7 days. This established technique produces over 90% ECM in culture and served as an *in vitro* model of equine corneal fibrosis.[31]

Cytotoxicity studies

Cellular viability was assessed using a trypan blue assay (Sigma-Aldrich, St. Louis, MO). ECFs were treated with PFD at concentrations of 0, 50, 100, 150, 200, and 300 μg/ml. Cells were trypsinized 48 h after initiation of respective treatment and suspended in 0.4% trypan blue solution (Invitrogen, Carlsbad, CA) and all blue and white cells were counted. Cellular viability was calculated as a percentage using viable ECF and total ECF counts acquired with a Neubauer hemocytometer.

The phenotypic changes in ECFs following the application of PFD were recorded using phase contrast microscopy (Leica, DMIL, Bannockburn, IL). ECF cultures grown in the presence or absence of varied concentrations of PFD (0, 50, 100, 150, 200, and 300 μg/ml) with or without TGFβ1 (1ng/ml) for 48 h were examined under a phase contrast microscope and images were captured using a digital imaging system (Leica DFC290, Bannockburn, IL) fitted to the microscope.

The response of PFD on ECF apoptosis was examined using a terminal deoxynucleotidyl transferase-mediated dUTP nick end labeling (TUNEL) assay. ECF cultures were grown in

the presence or absence of PFD (200 μg/ml) and TGFβ1 (1ng/ml) for 48 h, washed with phosphate buffered saline (PBS), and fixed with fresh 4% paraformaldehyde at room temperature for 20 min. The TUNEL assay was performed using a commercial ApopTag apoptosis detection kit (Chemicon International, Temecula, CA). Digital images were obtained using a fluorescent microscope (Leica DM 4000B, Bannockburn, IL) equipped with a CCD digital camera (SpotCam RT KE; Diagnostic Instruments Inc., Sterling Heights, MI).

Cellular proliferation

The effects of PFD on cellular proliferation were analyzed with a Cell Titer 96® Non-Radioactive Cell Proliferation Assay (MTT) following the manufacturer's instructions (Promega, Madison, WI). The MTT assay is a colorimetric assay which relies on the formation of a blue water-soluble formazan compound from the pale yellow tetrazolium salt 3-(4,5 dimethylthiazol-2-yl)-2,5-diphenyltetrazolium (MTT) after reduction by dehydrogenase enzymes in the mitochondria of living cells. An increase in the amount of MTT measured by absorbance is indicative of increased cellular proliferation. ECFs were seeded in a 96 well plate at a density of 5×10^3/well in 200 μl of MEM supplemented with 10% fetal bovine serum. After 24 h of incubation, PFD at a concentration of 200 μg/ml was then applied to each well for 12 h or 24 h. Following 12 h or 24 h treatment with 200 μg/ml PFD, 15 μl of Cell Titer 96® Non-Radioactive dye solution was added to each well for 4 h. Solubilization solution/stop mix (100 μl/well) was then added to each well to solubilize the product. Sample absorbance was recorded at 570nm with an Epoch Microplate Spectrophotometer (BioTek, Winooski, VT).

Cellular migration

The effects of PFD on cellular migration were examined using an *in vitro* scratch assay.[32] Preparation of the assay involved the creation of a standardized, linear “scratch” in the cell culture monolayer prior to PFD application. Phase contrast microscopy was utilized at Time 0 (T_0) and regular intervals to evaluate cellular morphology and images were collected to determine the rate of migration for each group at selected time points. ECFs were seeded in a 6 well plate with MEM supplemented with 10% fetal bovine serum and incubated overnight. Once ECFs reached 70% confluence, an identical gap was created on each plate with a p200 pipet tip. Cultures were washed with PBS to remove cellular debris and grown with or without TGFβ1 (1ng/ml) in the presence or absence of PFD (200 μg/ml) for 12 h, 24 h, 48 h, or 72 h. Images were collected using a phase-contrast microscope (Leica DMIL, Bannockburn, IL) equipped with an imaging system (Leica DFC290, Bannockburn, IL) at selected points. Comparative analysis of images from different time points and treatment groups was performed.

Immunofluorescence

Immunofluorescence staining was performed to confirm the presence of α-smooth muscle actin (αSMA), a marker for myofibroblasts, using mouse monoclonal primary αSMA antibody. Cultures were fixed with 4% paraformaldehyde, permeabilized with 0.025% triton for 15 min, incubated with 5% bovine serum albumin (BSA) for 30 min, and then incubated

with αSMA mouse monoclonal antibody (1:500 dilution; M0851; Dako, Carpinteria, CA) for 90 min at room temperature. Following incubation with the primary antibody, cells were washed twice with 1x PBS, and then incubated with Alexa 488 goat anti-mouse IgG secondary antibody (1:1000 dilution; A11001; Invitrogen, Carlsbad, CA) for 1 h, washed three times in 1x PBS, and mounted in Vectashield containing 4'-6'-Diamidino-2-phenylindole (DAPI) (Vector Laboratories Inc., Burlingame, CA). Immunostained cultures were viewed and photographed with a fluorescent microscope (Leica DM 4000B, Bannockburn, IL) equipped with a CCD digital camera (SpotCam RT KE; Diagnostic Instruments Inc., Sterling Heights, MI).

Immunoblotting

Cells were washed with PBS, lysed directly on plates with radioimmunoprecipitation assay protein lysis buffer (RIPA) containing protease inhibitor cocktail (Roche Applied Sciences, Indianapolis, IN). Samples were suspended in 4× NuPAGE LDS buffer containing a reducing agent (Invitrogen, Carlsbad, CA), centrifuged for 5 min at 10,000 ***g***, and then heated at 70 °C for 10 min. Protein samples were resolved by 4-10% SDS-PAGE on NuPAGE Novex Bis-Tris mini gels (Invitrogen, Carlsbad, CA) and transferred onto a 0.45-μm pore size PVDF membrane (Invitrogen, Carlsbad, CA). The PVDF membrane was incubated with αSMA (1:500 dilution; DAKO, Carpinteria, CA), or GAPDH primary antibodies (Santa Cruz Biotechnology Inc., Santa Cruz, CA) for 2 h followed by alkaline phosphatase conjugated anti-mouse secondary antibody for 1 h at room temperature. The PVDF blot was developed using the nitroblue tetrazolium/5-bromo-4-chloro-3-indolylphosphate (BCIP/NBT) method. Three separate western blots were performed and GAPDH was used as housekeeping for normalization of data.

Quantification using real-time PCR

Total RNA from ECF cultures receiving PFD treatment was extracted with an RNeasy kit (Qiagen, Valencia, CA) and converted to cDNA following manufacturer's instructions (Promega, Madison, WI). Real-time PCR was then performed using Step One Plus real-time PCR system (Applied Biosystems, Carlsbad, CA). A 20-μl reaction mixture containing 2 μl cDNA, 2 μl forward primer (200 nM), 2 μl reverse primer (200 nM), and 10 μl 2X SYBR green super mix (Bio-Rad Laboratories, Hercules, CA) was run at a universal cycle (95 °C for 10 min, 40 cycles at 95 °C for 15 s, and 60 °C for 60 s) following vendor's instructions. The forward and reverse αSMA primer sequences were TGG GTG ACG AAG CAC AGA GC and CTT CAG GGG CAA CAC GAA GC respectively. The β-actin gene was used as a housekeeping gene for the normalization of data. The forward and reverse primers of β-actin were CGG CTA CAG CTT CAC CAC CA and CGG GCA GCT CGT AGC TCT TC respectively. Cycle threshold (C_T) was used to detect increases in signal associated with exponential growth of PCR product during the log-linear phase. The relative gene expression was calculated using the following formula: $2^{-\Delta\Delta C_T}$, where C_T is a PCR cycle number at which the fluorescence meets the threshold in the amplification plot and ΔC_T is a subtraction product of target and housekeeping genes C_T values. The $2^{-\Delta\Delta C_T}$ formula is a method for determining relative target mRNA quantity in samples. Amplification efficiency for all templates used was validated by insuring that the difference between linear slopes for

all templates < 0.1. Three independent reactions were performed and the average (± standard deviation) results were calculated.

Quantification and statistical analysis

Immunocytochemistry data quantification was performed by counting αSMA and DAPI-positive cells in 10 randomly selected non-overlapping areas of fluorescent cultures at 200× magnification using a fluorescent microscope (Leica DM 4000B, Bannockburn, IL). All results are reported as mean ± standard deviation. Immunoblotting data was analyzed using Image J 1.38 X image analysis software (NIH, Bethesda, MD). The qRT-PCR data was analyzed using one-way ANOVA followed by Tukey's multiple comparison tests. A *P*-value of less than 0.01 was considered significant.

RESULTS

Pirfenidone safety

Figure-1 shows a dose-dependent effect of PFD treatment on the cellular viability of ECFs was determined by trypan blue exclusion assay. Tested concentrations of PFD up to 200 μg/ml did not cause significant change in the cellular viability of ECFs. PFD application at a concentration of 300 μg/ml caused a reduction in the population of viable ECFs at 48 h. We further evaluated the toxicity and safety of PFD by comparing cellular phenotype in PFD-treated and untreated ECFs. Figure-2 shows the effects of PFD-treatment (200 μg/ml) on ECFs phenotype. As evident from phase contrast microscopy images PFD, treatment (200 μg/ml) did not alter ECF phenotype 36 h following application (Fig. 2C) compared to corresponding controls (Fig. 2A-B). Similar results were noted 72 h after treatment of PFD 200 μg/ml (data not shown). The PFD dose of 300 μg/ml showed some phenotypic changes at tested times (data not shown) suggesting that this concentration was cytotoxic. Figure-3 shows results of TUNEL assay, which detects cellular apoptosis, and demonstrated the safety of PFD in this *in vitro* model. No detectable differences in TUNEL positive cells in PFD-treated (200 μg/ml) ECFs compared to untreated ECFs suggested that PFD application at a concentration of 200 μg/ml is safe to ECFs (Fig. 3).

Effect of Pirfenidone on cellular proliferation and cellular migration

The effects of PFD application on ECF proliferation were evaluated using a time dependent MTT assay. Treatment of ECFs with 200 μg/ml PFD resulted in a significant decrease in cellular proliferation (32 ± 3; $P < 0.001$) and (32 ± 4; $P < 0.001$) at 12 h and 24 h, respectively, compared to the untreated controls (Fig. 4). A scratch assay was used to determine the effects of PFD on TGFβ1-induced cellular migration across time.[32] TGFβ1 treatment (1ng/ml) substantially increased migration of ECFs compared to untreated control with partial apposition of the scratch edges being achieved after 72 h. Figure-5 shows the effects of PFD on ECF migration at 0 (A-C) and 72 (D-E) hours determined by scratch assay. The scratch wounds made at 0 h in 3 groups are shown in Figure 5A-C. At the 72 h, ECF cultured in the presence of PFD 200 μg/ml showed significantly reduced migration (F) than the untreated control (D) and TGFβ1-treated ECFs (E). The application of PFD at 200 μg/ml revealed significant inhibition of TGFβ1-induced cellular migration at 72 h (Fig. 5F; $P < 0.01$). The cellular migration plays a role in wound healing, and TGFβ1-induced ECF

migration has been recognized as an important characteristic of ECF differentiation to ECM.[12]

αSMA protein quantification by immunocytochemistry and immunoblotting

Results of immunofluorescence staining of αSMA demonstrating the TGFβ1-driven transformation of ECFs to ECMs are detailed in Fig. 6. Control ECFs not receiving TGFβ1 treatment are shown in Fig. 6a. Approximately 5-8% of the ECFs transformed to ECMs in the absence of TGFβ1 application (Fig 6A), which is known and consistent with previous publications. [33] Treatment of TGFβ1 (1ng/ml) to ECFs for 7 days under serum-free conditions stimulated the transdifferentiation of ECFs to ECMs as illustrated by the significant increase in αSMA+ cells (>94%; Fig. 6B) and treatment of 200 μg/ml PFD in ECFs grown in the presence of TGFβ1 significantly decreased αSMA+ cells (myofibroblasts) as evident from Fig. 6C. Quantification of αSMA immunocytochemical staining data is shown in Fig. 6D. TGFβ1 treatment (1ng/ml) of ECFs significantly increased level of αSMA (97.6 ± 3.2%; $P < 0.001$) compared to the untreated control (8.6 ± 2.8%). This TGFβ1-induced myofibroblast production was significantly reduced (85.8 ± 4.6%; $P < 0.001$) by the application of PFD at a concentration of 200 μg/ml. The western blotting of αSMA protein (Fig. 7) was consistent with our immunofluorescence quantitative analysis. Treatment of ECFs with TGFβ1 (1ng/ml) produced a significant increase (2.97-fold ± 0.25; $P < 0.001$) in αSMA protein compared to untreated controls. Furthermore, 200 μg/ml PFD treatment demonstrated a significant decrease in TGFβ1-induced αSMA protein expression (2.25-fold ± 0.125; $P < 0.001$).

αSMA RNA quantification by real-time qPCR

The relative expression of αSMA mRNA in the untreated negative control group, TGFβ1 treated group (1ng/ml), and 200 μg/ml PFD + TGFβ1 treatment group was quantified with real-time qPCR (Fig. 8). Treatment of ECFs with TGFβ1 (1ng/ml) produced a significant increase (3.01-fold ± 0.43; $P < 0.01$) in αSMA mRNA expression as compared to untreated controls. The 200 μg/ml PFD treatment significantly decreased (3.02-fold ± 0.41; $P < 0.01$) TGFβ1-mediated αSMA mRNA expression. The αSMA mRNA levels were similar between the 200 μg/ml PFD alone treatment and untreated control groups.

DISCUSSION

The pathogenesis of corneal fibrosis is an inherently complex physiological process owing to the combined upregulation of multiple cytokines including TGFβ, which is recognized as a significant driving force behind corneal fibrosis at the cellular level.[11, 33] Due to the role of TGFβ in transforming corneal keratocytes into fibroblasts and ultimately myofibroblasts, antagonizing TGFβ has become a proposed strategy for mitigating the deleterious fibrotic response which accompanies corneal wound healing. Our group has established an interest in developing novel therapeutic modalities that aim to neutralize the action of TGFβ and minimize corneal fibrosis in veterinary species.[34-38] Recent research has demonstrated the potential of gene therapy applications to mitigate TGFβ-driven corneal fibrosis including adenovirus-delivered soluble TGFβ receptor II (STGFRII), the overexpression of Smad7, and nanoparticle-mediated Decorin gene therapy.[36, 38, 39] Although these strategies

effectively down-regulate TGFβ, they require specialized delivery systems for use in clinical veterinary ophthalmology at this time. We hypothesize that the antagonism of TGFβ through the application of a topical anti-fibrotic compound such as Pirfenidone is an effective approach to preventing and treating equine corneal fibrosis that could be replicated with ease in a clinical setting.

PFD has been demonstrated to inhibit a variety of cytokines involved in wound healing including connective tissue growth factor (CTGF), platelet derived growth factor (PDGF), tumor necrosis factor (TNF), and transforming growth factor beta (TGFβ).[22, 23, 25] Of particular interest to our group is the ability of PFD to down-regulate TGFβ and subsequently reduce fibrotic changes in healing ocular tissues. PFD was originally shown to be an anti-fibrotic agent and after being examined in greater detail for idiopathic pulmonary fibrosis, it exhibited substantial anti-inflammatory, anti-fibrotic, and anti-hydroxyl radical properties.[20, 25, 26] The results gleaned from *in vitro* and *in vivo* studies prompted additional evaluation of PFD in experimental models of hepatic, renal, and cardiac fibrosis.[21, 22, 26, 40]

In vision science research, PFD application has been shown to inhibit the proliferation, migration, and collagen contraction of human Tenon's fibroblasts *in vitro* while also reducing post-operative fibrosis in experimental glaucoma surgery.[24, 27] PFD has been shown to decrease fibrosis *in vivo* following strabismus surgery in a rabbit model.[23] PFD exhibits significant anti-fibrotic effects on fibroblasts isolated from patients with thyroid-associated ophthalmopathy while also inhibiting the TGFβ-induced fibrogenesis of retinal pigmented epithelial cells.[28, 41] PFD has been recently shown to decrease TGFβ-induced collagen synthesis and prevent the formation of myofibroblasts in an *in vitro* model of rat corneal fibrosis. In a complimentary *in vivo* study, PFD loaded poly (lactide-co-glycolide) (PLGA) nanoparticles significantly improved corneal wound healing and prevented corneal fibrosis following a controlled alkali burn in a rat model.[42]

To the authors' knowledge, this work represents the first examination of the anti-fibrotic effects of PFD in treating equine corneal fibrosis. The present study demonstrated that topical administration of PFD prevents corneal fibrosis through the inhibition of TGFβ-driven fibroblast migration and myofibroblast formation. PFD is likely to be beneficial in the control of corneal fibrosis occurring secondary to corneal insult in equine patients in clinical settings. Further examination is required to determine the optimal dosage of PFD for the treatment of equine corneal fibrosis in clinical patients as well as to determine the effectiveness of treating an established fibrotic corneal lesion. *In vivo* studies are warranted.

Acknowledgements

This research was funded mainly by the Phi Zeta Research Grant from the College of Veterinary Medicine, University of Missouri (MKF), the Ruth M. Kraeuchi Missouri Endowed Chair Professor Veterinary Ophthalmology Fund (RRM), and partially by the R01EY017294 National Eye Institute, National Institutes of Health, Bethesda (RRM), and the 1I01BX000357 Veteran Health Affairs Merit Grant, Washington DC (RRM).

References

1. Michau TM, Schwabenton B, Davidson MG, et al. Superficial nonhealing corneal ulcers in horses: 23 cases (1989-2003). Veterinary Ophthalmology. 2003; 6:291–297. [PubMed: 14641825]
2. Haber M, Cao Z, Panjwani N, et al. Effects of growth factors (EGF, PDGF-BB and TGF-beta 1) on cultured equine epithelial cells and keratocytes: implications for wound healing. Veterinary Ophthalmology. 2003; 6:211–217. [PubMed: 12950652]
3. Nasisse MP, Nelms S. Equine ulcerative keratitis. Veterinary Clinics of North America: Equine Practice. 1992; 8:537–555.
4. Boote C, Dennis S, Newton RH, et al. Collagen fibrils appear more closely packed in the prepupillary cornea: optical and biomechanical implications. Investigative Ophthalmology & Visual Science. 2003; 44:2941–2948. [PubMed: 12824235]
5. Conrad GW, Funderburgh JL. Eye development and the appearance and maintenance of corneal transparency. Transactions of the Kansas Academy of Science. 1992; 95:34–38. [PubMed: 11537981]
6. Maurice DM. The transparency of the corneal stroma. Vision Research. 1970; 10:107–108. [PubMed: 5435007]
7. Mohan RR, Hutcheon AE, Choi R, et al. Apoptosis, necrosis, proliferation, and myofibroblast generation in the stroma following LASIK and PRK. Experimental Eye Research. 2003; 76:71–87. [PubMed: 12589777]
8. Wilson SE, Mohan RR, Ambrosio R, et al. The corneal wound healing response: cytokine-mediated interaction of the epithelium, stroma, and inflammatory cells. Progress in Retinal and Eye Research. 2001; 20:625–637. [PubMed: 11470453]
9. Maltseva O, Folger P, Zekaria D, et al. Fibroblast growth factor reversal of the corneal myofibroblast phenotype. Investigative Ophthalmology & Visual Science. 2001; 42:2490–2495. [PubMed: 11581188]
10. Margadant C, Sonnenberg A. Integrin-TGF-beta crosstalk in fibrosis, cancer and wound healing. EMBO Reports. 2010; 11:97–105. [PubMed: 20075988]
11. Tandon A, Tovey JC, Sharma A, et al. Role of transforming growth factor beta in corneal function, biology, and pathology. Current Molecular Medicine. 2010; 10:565–578. [PubMed: 20642439]
12. Myrna KE, Pot SA, Murphy CJ. Meet the corneal myofibroblast: the role of myofibroblast transformation in corneal wound healing and pathology. Veterinary Ophthalmology. 2009; 12:25–27. [PubMed: 19891648]
13. Jester JV, Huang J, Barry-Lane PA, et al. Transforming growth factor(beta)-mediated corneal myofibroblast differentiation requires actin and fibronectin assembly. Investigative Ophthalmology & Visual Science. 1999; 40:1959–1967. [PubMed: 10440249]
14. Jester JV, Huang J, Fisher S, et al. Myofibroblast differentiation of normal human keratocytes and hTERT, extended-life human corneal fibroblasts. Investigative Ophthalmology & Visual Science. 2003; 44:1850–1858. [PubMed: 12714615]
15. Jester JV, Petroll WM, Cavanagh HD. Corneal stromal wound healing in refractive surgery: the role of myofibroblasts. Progress in Retinal and Eye Research. 1999; 18:311–356. [PubMed: 10192516]
16. Cordeiro MF, Mead A, Ali RR, et al. Novel antisense oligonucleotides targeting TGF-beta inhibit in vivo scarring and improve surgical outcome. Gene Therapy. 2003; 10:59–71. [PubMed: 12525838]
17. Jester JV, Barry-Lane PA, Petroll WM, et al. Inhibition of corneal fibrosis by topical application of blocking antibodies to TGF beta in the rabbit. Cornea. 1997; 16:177–187. [PubMed: 9071531]
18. Netto MV, Mohan RR, Ambrosio R, et al. Wound healing in the cornea: a review of refractive surgery complications and new prospects for therapy. Cornea. 2005; 24:509–522. [PubMed: 15968154]
19. Thom SB, Myers JS, Rapuano CJ, et al. Effect of topical anti-transforming growth factor-beta on corneal stromal haze after photo-refractive keratectomy in rabbits. Journal of Cataract and Refractive Surgery. 1997; 23:1324–1330. [PubMed: 9423903]

20. Antoniu SA. Pirfenidone for the treatment of idiopathic pulmonary fibrosis. Expert Opinion on Investigational Drugs. 2006; 15:823–828. [PubMed: 16787145]
21. Di Sario A, Bendia E, Macarri G, et al. The anti-fibrotic effect of pirfenidone in rat liver fibrosis is mediated by downregulation of procollagen α1(I), TIMP-1 and MMP-2. Digestive and Liver Disease. 2004; 36:744–751. [PubMed: 15571005]
22. Hewitson TD, Kelynack KJ, Tait MG, et al. Pirfenidone reduces in vitro rat renal fibroblast activation and mitogenesis. Digestive and Liver Disease. 2001; 14:453–460.
23. Jung KI, Choi JS, Kim HK, et al. Effects of an anti-transforming growth factor-beta agent (pirfenidone) on strabismus surgery in rabbits. Current Eye Research. 2012; 37:770–776. [PubMed: 22671031]
24. Lin X, Yu M, Wu K, et al. Pirfenidone inhibits proliferation, migration, and collagen contraction of human tenon's fibroblasts in vitro. Investigative Ophthalmology & Visual Science. 2009; 50:3763–3770. [PubMed: 19264889]
25. Oku H, Shimizu T, Kawabata T, et al. Antifibrotic action of pirfenidone and prednisolone: different effects on pulmonary cytokines and growth factors in bleomycin-induced murine pulmonary fibrosis. European Journal of Pharmacology. 2008; 590:400–408. [PubMed: 18598692]
26. Schaefer CJ, Ruhrmund DW, Pan L, et al. Antifibrotic activities of pirfenidone in animal models. European Respiratory Review. 2011; 20:85–97. [PubMed: 21632796]
27. Zhong H, Sun G, Lin X, et al. Evaluation of pirfenidone as a new postoperative antiscarring agent in experimental glaucoma surgery. Investigative Ophthalmology & Visual Science. 2011; 52:3136–3142. [PubMed: 21330661]
28. Choi K, Lee K, Ryu SW, et al. Pirfenidone inhibits transforming growth factor-beta1-induced fibrogenesis by blocking nuclear translocation of Smads in human retinal pigment epithelial cell line ARPE-19. Molecular Vision. 2012; 18:1010–1020. [PubMed: 22550395]
29. Sun G, Lin X, Zhong H, et al. Pharmacokinetics of pirfenidone after topical administration in rabbit eye. Molecular Vision. 2011; 17:2191–2196. [PubMed: 21866212]
30. Azuma A. Pirfenidone treatment of idiopathic pulmonary fibrosis. Therapeutic Advances in Respiratory Disease. 2012; 6:107–114. [PubMed: 22333982]
31. Buss DG, Giuliano EA, Sharma A, et al. Isolation and cultivation of equine corneal keratocytes, fibroblasts and myofibroblasts. Veterinary Ophthalmology. 2010; 13:37–42. [PubMed: 20149174]
32. Liang CC, Park AY, Guan JL. In vitro scratch assay: a convenient and inexpensive method for analysis of cell migration in vitro. Nature Protocols. 2007; 2:329–333.
33. Jester JV, Huang J, Petroll WM, et al. TGFbeta induced myofibroblast differentiation of rabbit keratocytes requires synergistic TGFbeta, PDGF and integrin signaling. Experimental Eye Research. 2002; 75:645–657. [PubMed: 12470966]
34. Bosiack AP, Giuliano EA, Gupta R, et al. Efficacy and safety of suberoylanilide hydroxamic acid (Vorinostat) in the treatment of canine corneal fibrosis. Veterinary Ophthalmology. 2012; 15:307–314. [PubMed: 22212187]
35. Buss DG, Sharma A, Giuliano EA, et al. Efficacy and safety of mitomycin C as an agent to treat corneal scarring in horses using an in vitro model. Veterinary Ophthalmology. 2010; 13:211–218. [PubMed: 20618797]
36. Donnelly KS, Giuliano EA, Sharma A, et al. Decorin-PEI nanoconstruct attenuates equine corneal fibroblast differentiation. Veterinary Ophthalmology. 2013; 16:1–8.
37. Gupta R, Yarnall BW, Giuliano EA, et al. Mitomycin C: a promising agent for the treatment of canine corneal scarring. Veterinary Ophthalmology. 2011; 14:304–312. [PubMed: 21929607]
38. Sharma A, Rodier JT, Tandon A, et al. Attenuation of corneal myofibroblast development through nanoparticle-mediated soluble transforming growth factor-beta type II receptor (sTGFbetaRII) gene transfer. Molecular Vision. 2012; 18:2598–2607. [PubMed: 23112572]
39. Ka SM, Yeh YC, Huang XR, et al. Kidney-targeting Smad7 gene transfer inhibits renal TGF-beta/MAD homologue (SMAD) and nuclear factor kappaB (NF-kappaB) signalling pathways, and improves diabetic nephropathy in mice. Diabetologia. 2012; 55:509–519. [PubMed: 22086159]
40. Shi Q, Liu X, Bai Y, et al. In vitro effects of pirfenidone on cardiac fibroblasts: proliferation, myofibroblast differentiation, migration and cytokine secretion. PLOS ONE. 2011; 6

41. Kim H, Choi YH, Park SJ, et al. Antifibrotic effect of pirfenidone on orbital fibroblasts of patients with thyroid-associated ophthalmopathy by decreasing TIMP-1 and collagen levels. Investigative Ophthalmology & Visual Science. 2010; 51:3061–3066. [PubMed: 20053983]

42. Chowdhury S, Guha R, Trivedi R, et al. Pirfenidone nanoparticles improve corneal wound healing and prevent scarring following alkali burn. PLOS ONE. 2013; 8

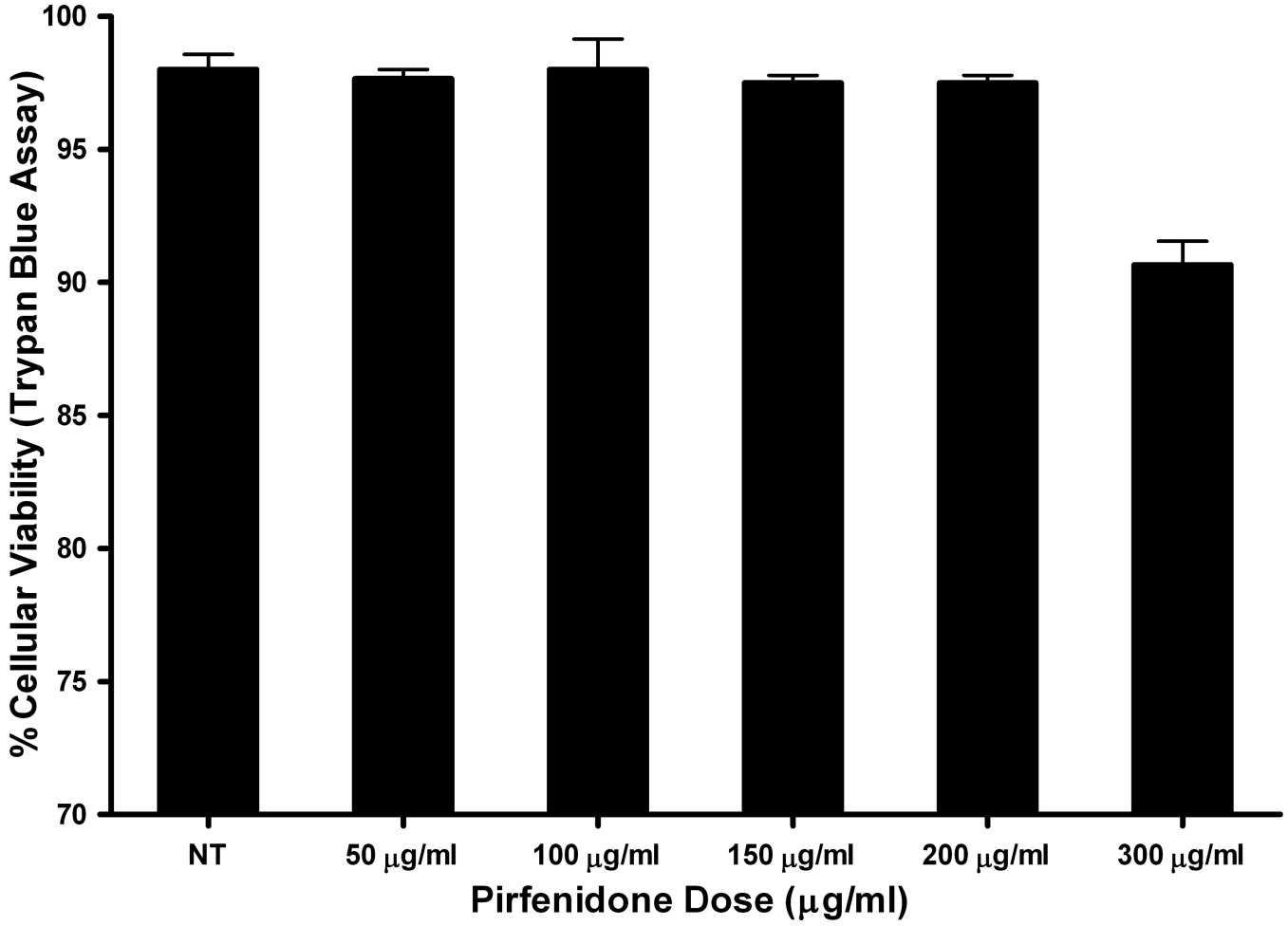

Figure 1.

A bar graph showing the cellular viability as determined by trypan blue assay to demonstrate the dose-dependent effect of Pirfenidone (PFD) treatment on equine corneal fibroblasts (ECF). Doses of 200 μg/ml PFD or less did not alter cellular viability. However, PFD dose of 300 μg/ml demonstrated mild cellular toxicity.

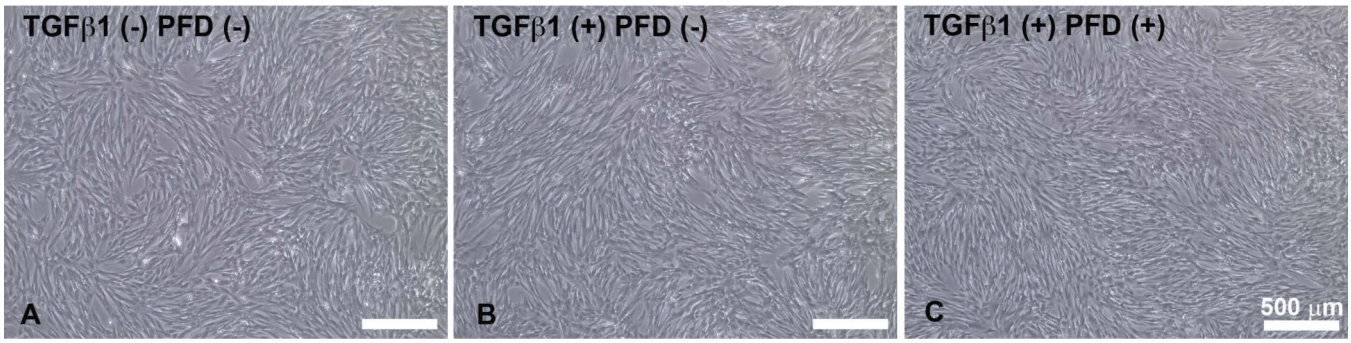

Figure 2.

A composite phase-contrast microscopy image showing untreated control, TGFβ1-treated control, and TGFβ1 + 200 μg/ml PFD treatment groups taken 36 hours after initiation of PFD treatment. No alterations in cellular morphology were observed. Scale bar denotes 500 μm.

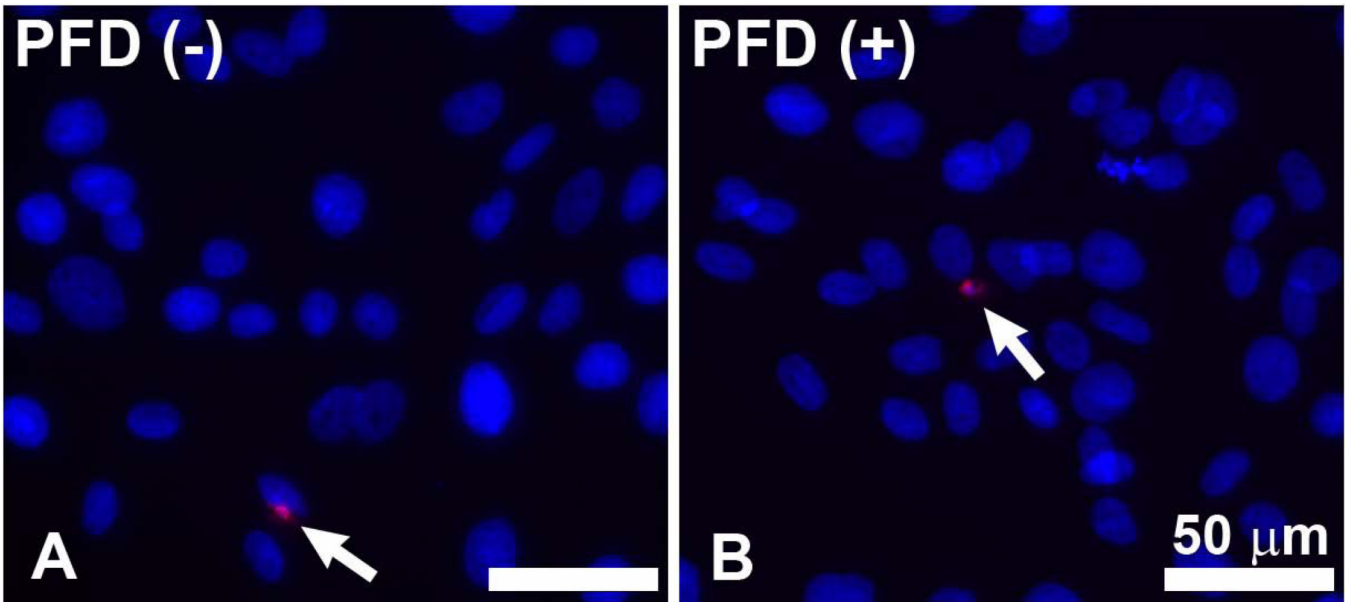

Figure 3.

Representative image of TUNEL assay results detecting apoptosis of ECFs in the untreated control group and in ECFs treated with TGFβ1 + 200 μg/ml PFD for 24 h. No detectable differences were observed between treated and control groups. Scale bar denotes 50 μm.

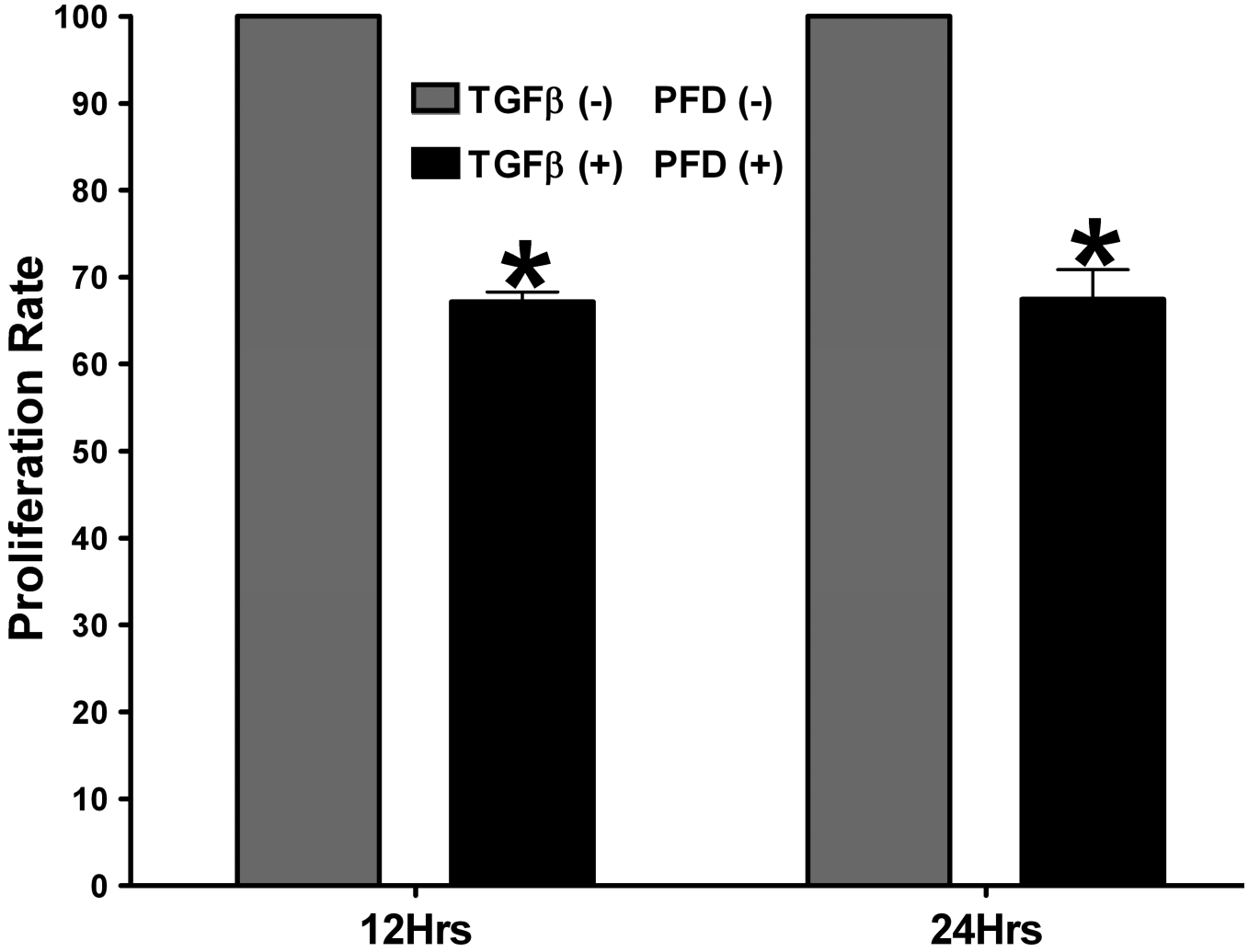

Figure 4.

Results of MTT Cellular Proliferation Assay. ECM proliferation was significantly reduced with TGFβ1 + 200 μg/ml PFD treatment as compared to the TGFβ1-treated control groups at 12 h and 24 h. Error bars indicate standard error. *denotes $P < 0.001$ (TGFβ1-treated control versus TGFβ1 + PFD treatment)

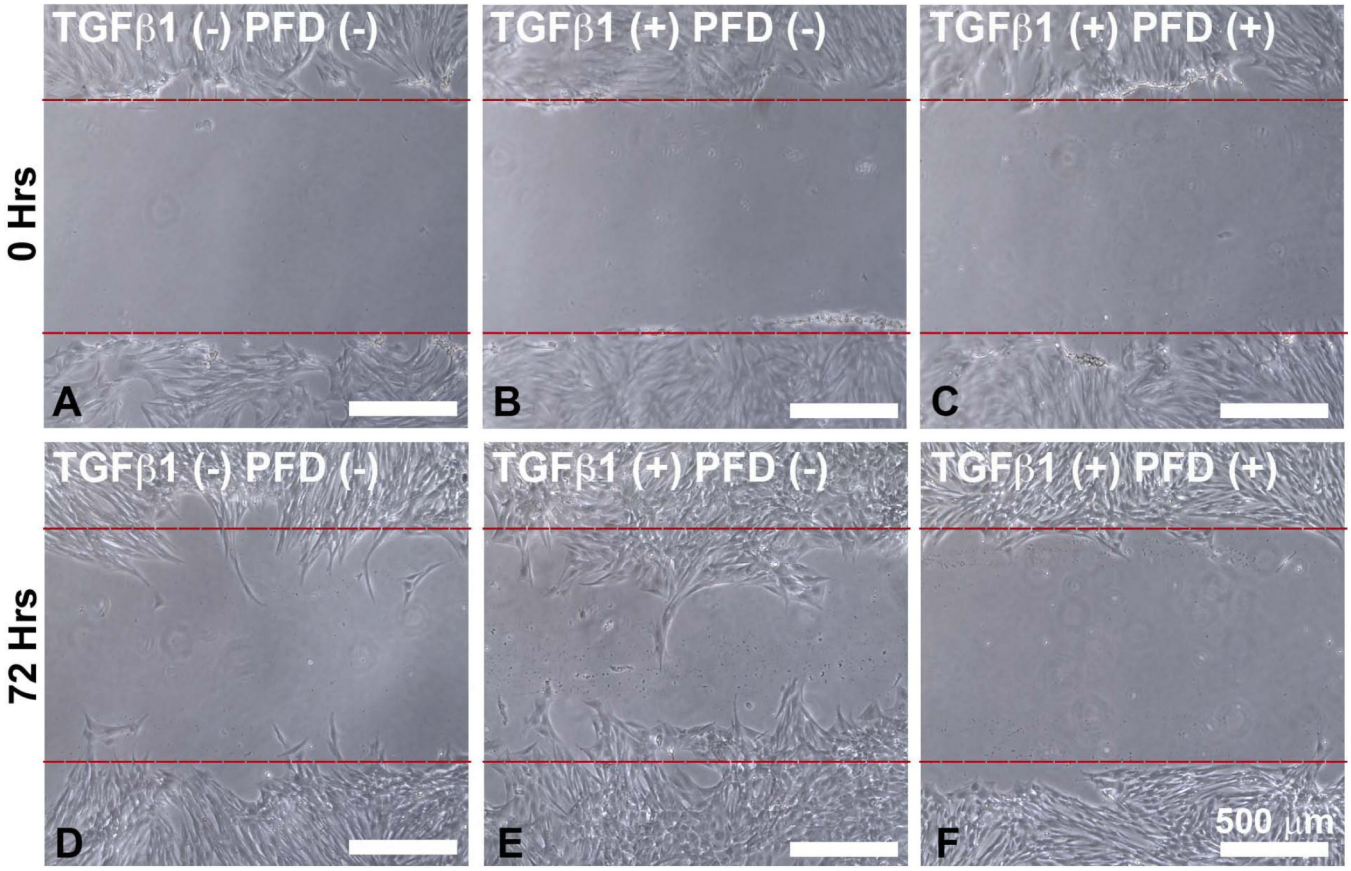

Figure 5.

Cell Migration Scratch Assay. Composite phase-contrast microscopy image showing ECF taken 72 hours after initiation of 200 μg/ml PFD treatment. PFD treatment effectively reduced cellular migration as compared to the TGFβ1-treated control group. Scale bar denotes 500 μm.

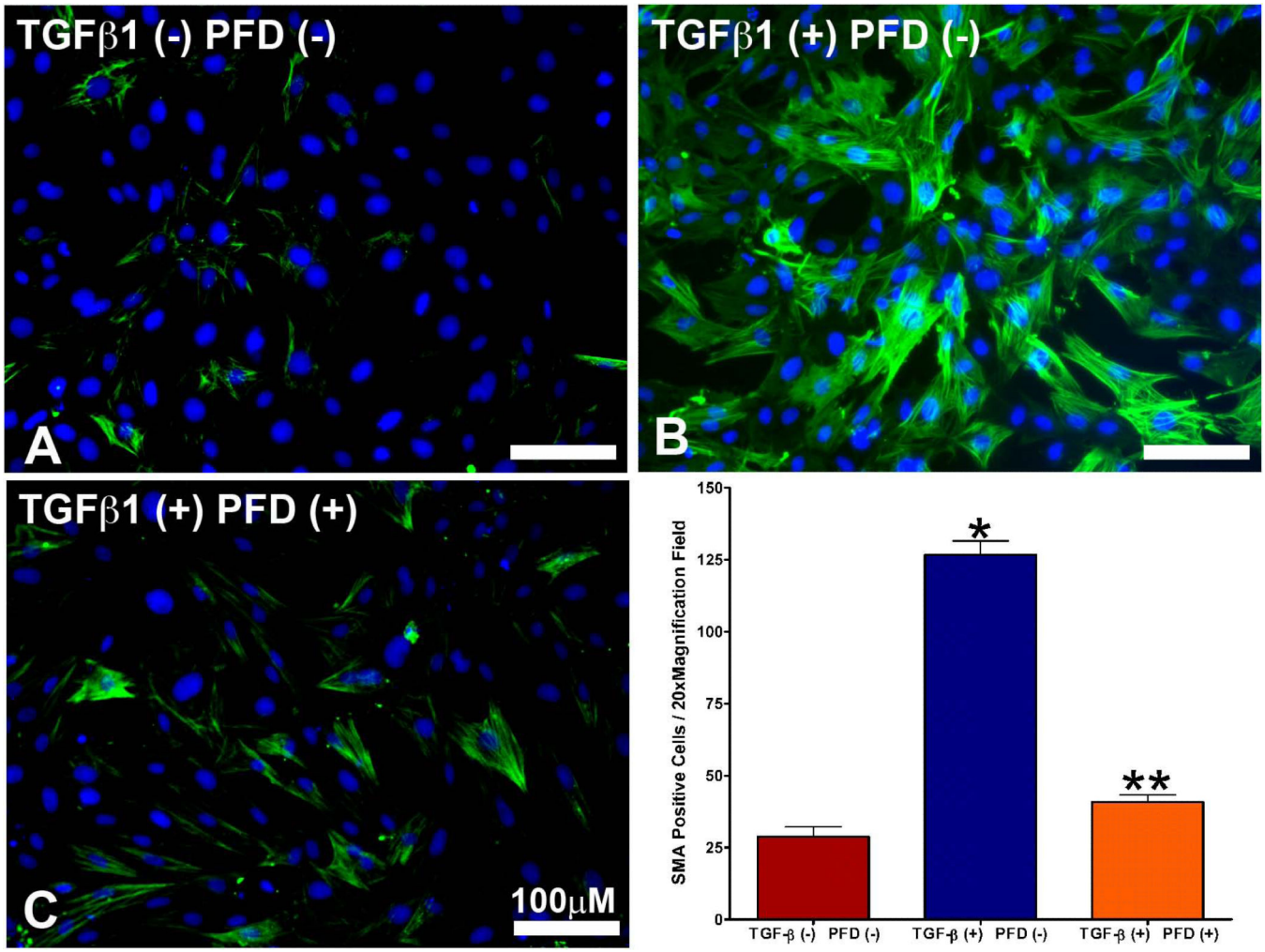

Figure 6.

a. Immunocytochemical staining using the myofibroblast marker αSMA antibody (green) in untreated control ECFs.

Figure 6b. TGFβ1 treatment (1ng/ml) showed increased myofibroblast formation compared to untreated control ECFs.

Figure 6c. The 200 μg/ml PFD treatment showed significant reduction in TGFβ1-induced myofibroblast formation. Nuclei are stained blue with DAPI. Scale bar denotes 100 μm.

Figure 6d. Immunocytochemical staining quantification of αSMA. TGFβ1 treatment of ECFs produced a significantly higher level of αSMA staining when compared to the untreated control group. Treatment with 200 μg/ml PFD significantly decreased TGFβ1-induced myofibroblast formation. Error bars indicate standard error.

* denotes $P < 0.001$ (untreated control versus TGFβ1 treatment)

** denotes $P < 0.001$ (TGFβ1 treatment versus TGFβ1 + PFD treatment).

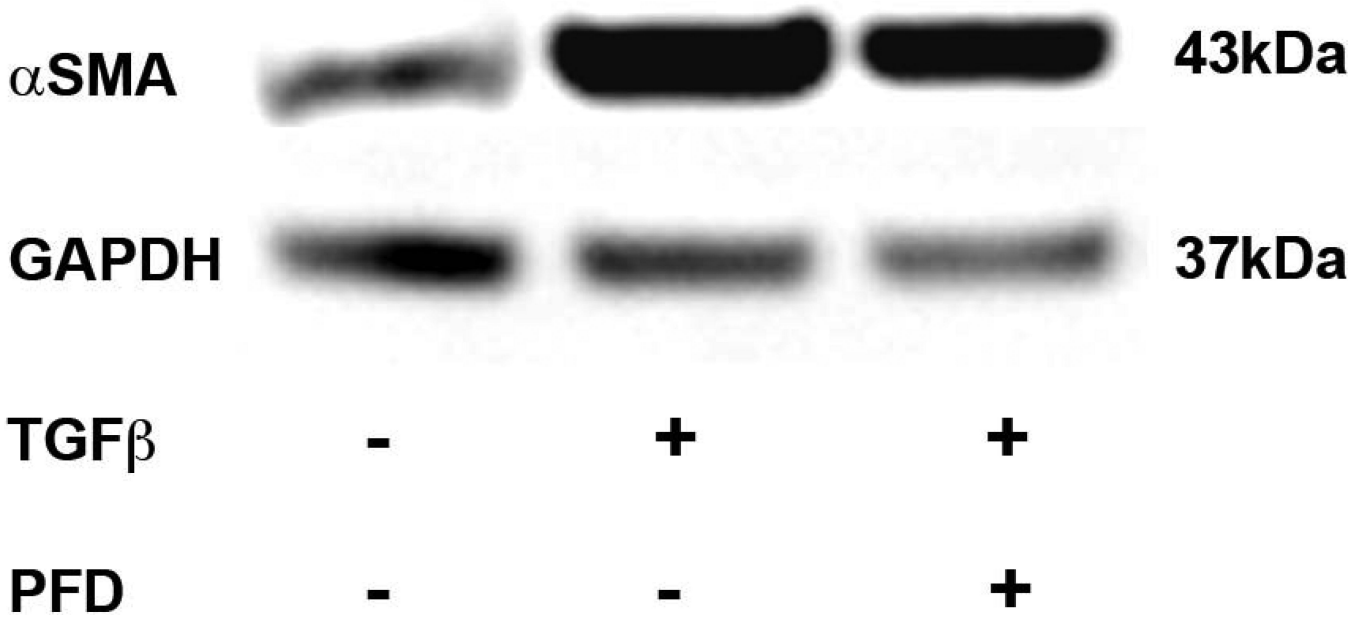

Figure 7.

Immunoblot analysis demonstrating quantitative measurement of αSMA in ECF cultures treated with or without TGFβ1 (1ng/ml) and 200 μg/ml PFD. Equal quantity of protein (30μg) was loaded in each lane. Left lane is untreated control. Cell lysates prepared from TGFβ1-treated cells were loaded in center lane. TGFβ1 + PFD-treated cell lysates were loaded in right lane. GAPDH was used as a housekeeping gene. The 200 μg/ml PFD treatment showed significant decrease in TGFβ1-induced myofibroblast formation. Error bars indicate standard error.

* denotes $P < 0.001$ (untreated control versus TGFβ1 treatment)

** denotes $P < 0.001$ (TGFβ1 treatment versus TGFβ1 + PFD treatment).

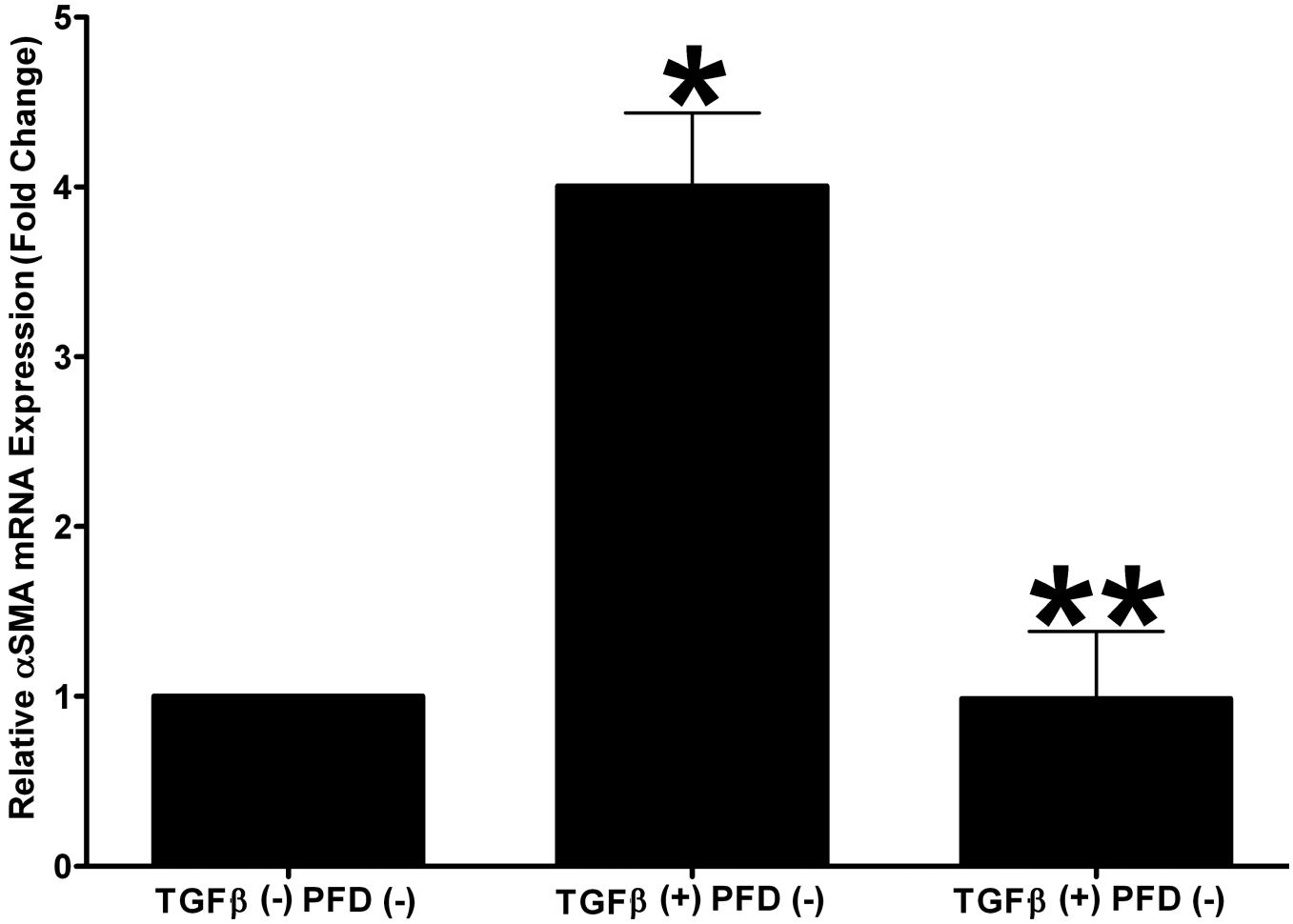

Figure 8.

Quantitative real-time PCR results demonstrating the relative expression of αSMA mRNA. TGFβ1 treatment (1ng/ml) induced significant αSMA formation (four-fold) in myofibroblasts and 200 μg/ml PFD treatment significantly decreased TGFβ1-induced myofibroblast formation. Error bars indicate standard error.

* denotes $P < 0.001$ (untreated control versus TGFβ1 treatment)

** denotes $P < 0.001$ (TGFβ1 treatment versus TGFβ1 + PFD treatment).